

Training Generative Networks with general Optimal Transport distances.

Vaios Laschos*

Jan Tinapp*

Klaus Obermayer*

December 21, 2024

Abstract

We propose a new algorithm that uses an auxiliary Neural Network to calculate the transport distance between two data distributions and export an optimal transport map. In the sequel we use the aforementioned map to train Generative Networks. Unlike WGANs, where the Euclidean distance is implicitly used, this new method allows to use any transportation cost function that can be chosen to match the problem at hand. More specifically, it allows to use the squared distance as a transportation cost function, giving rise to the Wasserstein-2 metric for probability distributions, which has rich geometric properties that result in fast and stable gradients descends. It also allows to use image centered distances, like the Structure Similarity index, with notable differences in the results.

1 Introduction

1.1 The birth of GANs

In the seminal work of Goodfellow et al. [9], a ground breaking approach for training Generative Networks (GNs) was proposed. GNs try to generate new data given some training data x . This is achieved by treating the data as samples from an unknown empirical probability function \mathbb{P}_r and fitting a model \mathbb{P}_θ to give an estimate for this function. By drawing samples from \mathbb{P}_θ , new data points can be generated that resemble the original dataset. The approach in [9] proposes to use two neural networks one of which is the *generator* $G(z)$ and the other acts as a *discriminator* $D(x)$. The *generator* represents the model \mathbb{P}_θ , while the *discriminator* gives a differentiable measure of how similar \mathbb{P}_θ is to \mathbb{P}_r . To train the *generator* the two networks participate in a two-player minimax game where the *discriminator* is maximizing the probability to detect if data shown to it comes from the *generator* or the training dataset. The *generator* is trying to fool the *discriminator* by minimizing the probability of generated data being detected. To train the networks the value function

*Fakultät Elektrotechnik und Informatik, and Bernstein Center for Computational Neuroscience, Technische Universität Berlin, Marchstr. 23, 10587, Berlin, Germany (vaios.laschos@tu-berlin.de, jan.tinapp@tu-berlin.de, klaus.obermayer@mailbox.tu-berlin.de).

$\min_G \max_D V(D, G) = \mathbb{E}_{x \sim \mathbb{P}_r}[\log D(x)] + \mathbb{E}_{x \sim \mathbb{P}_\theta}[\log(1 - D(x))]$ is used by switching between taking the gradient with respect to the weights in $G(x)$ and $D(x)$.

As it is explained in [9], the *discriminator* provides an error function for the *generator*. A fully trained *discriminator* will provide as a cost the relative entropy of the generated distribution \mathbb{P}_θ with respect to the real distribution \mathbb{P}_r . However relative entropy is a good metric distance for two distributions, only when they have the same support. If the distributions have different supports the error function cannot provide any information for the points charged by \mathbb{P}_θ and not by \mathbb{P}_r . In practice this means that if the *discriminator* is well trained then it does not provide a gradient for the *generator* to learn, which result to the phenomenon of mode collapse. To fix that, researchers suggested various technical solutions, among them being the introduction of vanishing noise, since by adding some noise, the two distributions have always the same support. However, most of these solutions were producing other problems in return.

1.2 The introduction of WGANs

To deal with the issues that the original GANs exhibited, various new approaches were introduced, with the most noticeable being the Wasserstein GAN [1] by Arjovsky et. al. that views the problem as an optimal transport task. In this approach the Wasserstein-1 distance between samples from the real distribution and samples from the current model is approximated and then minimized by changing the *generator* weights. In order to find the gradient to change the model, a differentiable way of calculating the Wasserstein-1 distance is required. This issue is resolved by introducing a neural network, the *critic*, that gets trained to approximate the Wasserstein distance between samples from both distributions.

To adapt the model with respect to the distance, the following formula was used:

$$W_1(\mathbb{P}_\theta, \mathbb{P}_r) := \sup_{\psi \in \text{Lip}_1} \left\{ \int \psi d\mathbb{P}_\theta - \int \psi d\mathbb{P}_r \right\}. \quad (1.1)$$

where $\psi(x)$ is the output from the *critic* and $\|\psi\|_L \leq 1$ constrains it to be 1-Lipschitz.

1.3 A new approach

The simplicity for calculating the Wasserstein-1 distance comes from its dual formulation (1.1). One needs only a function, that can be encoded by the *critic* Neural Network, to express ψ in (1.1), which in the sequel can be used to train the *generator*. At the same time, if one tries to apply different transportation costs, then a nice formula like this does not exist anymore. However, when one trains the *generator* with the Euclidian distance as an underlying transport cost, then the *generator* produces new elements that are closed to the old ones with respect to that distance. Something like that may not be optimal, when one wants to deal with distribution of data that have a different intrinsic metric. For example, when one tries to measure distance between two images, the Euclidean distance between pixels may not be the right choice as Figure 1 indicates. In this paper we propose a method for calculating the optimal transport distance between two distributions, with arbitrary transport cost. This way, the "data" manifold that the *generator* produces can fit

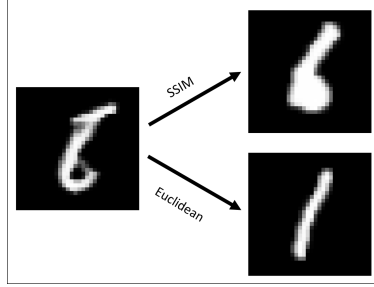


Figure 1: The closest real point to a generated one, in respect to SSIM and the Euclidean distance respectively.

better to the data distribution. Also as we will argue in the sequel, our method allows to optimize the training to any desirable degree, restricted only by processing power, in order to be sure that there is no mode collapse. **We would like to emphasize at this point, that the method that we propose does not train like other GANs and it is not a variation of them.**

The layout of the paper is the following. First we have a discussion on optimal transportation distances, and a short literature review on the special case of the Wasserstein-1 distance. We proceed with a mathematical analysis of our method, to which we will refer from now on as the **Assignment method**. Next, we provide a heuristic visual explanation of the difference in training between WGANs and our method. Finally we provide our experimental results and we enumerate the strengths and drawbacks of the Assignment method.

2 Optimal transportation distances

For the sequel, let $(\mathcal{X}, d_{\mathcal{X}})$ be a compact metric space. We will denote by $\mathfrak{M}(\mathcal{X})$ the space of all nonnegative and finite Borel measures on \mathcal{X} endowed with the weak topology induced by the duality with the continuous and bounded functions of $C_b(\mathcal{X})$. The set $\mathcal{P}(\mathcal{X}) \subset \mathfrak{M}(\mathcal{X})$ is the subset of probability measures. Let finally $c : \mathcal{X} \times \mathcal{X} \rightarrow \mathbb{R}^+$, a transportation “cost” function that is continuous with respect to the distance $d_{\mathcal{X}}$. For two measures μ, ν , a transport plan between μ and ν is a measure $Q \in \mathcal{P}(\mathcal{X} \times \mathcal{X})$ with marginals $\mu := \pi_{\sharp}^0 Q, \nu := \pi_{\sharp}^1 Q$. In the last line, we applied the following definition.

Definition 2.1 *If $\mu \in \mathcal{P}(\mathcal{X})$ and $T : \mathcal{X} \rightarrow \mathcal{Y}$ is a Borel map, $T_{\sharp}\mu$ will denote the push-forward measure on \mathcal{Y} , defined by*

$$T_{\sharp}\mu(B) := \mu(T^{-1}(B)) \quad \text{for every Borel set } B \subset \mathcal{Y}. \quad (2.1)$$

Now we define the optimal transport distance between two measures μ, ν .

Definition 2.2 *Given a couple of measures $\mu, \nu \in \mathcal{P}(\mathcal{X})$, their c -Optimal Transportation distance \mathcal{T}_c is defined by*

$$\mathcal{T}_c(\mu, \nu) := \min_{Q \in \mathcal{P}(\mathcal{X} \times \mathcal{X})} \left\{ \iint c(x, y) dQ(x, y) \mid \pi_{\sharp}^0 Q = \mu \wedge \pi_{\sharp}^1 Q = \nu \right\}. \quad (2.2)$$

For the case where $c = d_{\mathcal{X}}$, we recover the so called Monge-Kantorovich distance or Wasserstein-1, i.e. $W_1 = \mathcal{T}_{d_{\mathcal{X}}}$. Also when $c = d_{\mathcal{X}}^2$, the square root of $\mathcal{T}_{d_{\mathcal{X}}^2}$, gives the Wasserstein-2 distance, i.e. $W_2 = \sqrt{\mathcal{T}_{d_{\mathcal{X}}^2}}$. In the sequel, we are going to denote the set of all integrable functions with respect to some probability measure μ , with $\mathcal{L}(\mu)$. We are also going to use the notation $supp(\mu)$ for the support of μ . From [13], we have:

Theorem 2.3 (Dual formulation) *For $\mu, \nu \in \mathcal{P}(\mathcal{X})$, we have*

$$\begin{aligned} \mathcal{T}_c(\mu, \nu) &:= \sup_{\phi, \psi \in C_b(\mathcal{X})} \left\{ \int \phi \, d\mu(x) - \int \psi \, d\nu(y) \mid \phi(x) + \psi(y) \leq c(x, y) \right\} \\ &= \sup_{\psi \in C_b(\mathcal{X})} \left\{ \int \psi^c \, d\mu(x) - \int \psi \, d\nu(y) \mid \psi^c(x) = \inf_{y \in \mathcal{X}} \{c(x, y) + \psi(y)\} \right\} \\ &= \sup_{\psi \in C_b(\mathcal{X})} \left\{ \int \psi^{supp(\nu), c} \, d\mu(x) - \int \psi \, d\nu(y) \mid \psi^{supp(\nu), c}(x) = \inf_{y \in supp(\nu)} \{c(x, y) + \psi(y)\} \right\}. \end{aligned} \tag{2.3}$$

2.1 The case of the Wasserstein-1 distance: from weight clipping to the two-step approximation method

In [2], the authors suggest the use of the Wasserstein-1 distance as an error function for training GANs. In order to implement the Wasserstein-1 distance, the authors used a special form of the dual formulation (2.3) that holds only for the case of the Wasserstein-1 distance. Specifically, they used the fact that if ψ is a Lipschitz function with Lipschitz constant smaller than one, then ψ^c is equal to ψ . This gives rise to the formula

$$W_1(\mu, \nu) := \sup_{\psi \in \text{Lip}_1} \left\{ \int \psi \, d\mu(x) - \int \psi \, d\nu(y) \right\}. \tag{2.4}$$

In order to implement this form of the distance, one had to establish that during the training procedure the function ψ has to have Lipschitz constant of less than one. In order to achieve that, they introduced the method known as *weight clipping*, where any time a weight exceeds a specific limit, it is reduced so it can retain its Lipschitz constant. However, this first approach, although quite plausible, did not have any rigorous mathematical justification, and it is known to cause issues like stacking or instability of the learning process, as it was pointed out in [10]. Following [2], in several publications, authors tried to fix, improve or replace this method. Among the most notable papers, in [10] the authors propose a method to stabilize the gradient. More recently, in [11] the authors propose to first solve a linear programming problem and then use the solution to train the *critic* to mimic the solution. Even more the method [11] allows for more general transportation costs, provided that they satisfy the triangular inequality. However, even in the method proposed in [11], the squared distance is not applicable, since it does not satisfy the triangular inequality. Furthermore, this method requires a process that is outside the training circle, making it difficult to compare efficiency with established methods.

3 Mathematical justification for a new network type and error function: The Assignment method

Before we proceed, we will make the following assumption for the cost c

Assumption 3.1 *For every $x \in \mathcal{X}$, the level sets of $c(x, \cdot)$, ie $\mathcal{X}_{x,a} = \{y \in \mathcal{X} : c(x, y) = a\}$, have Lebesgue measure zero.*

We note that it is simple to show that the assumption holds true for all norms.

Let now ψ_w denote the function that corresponds to the Assigning network (imagine that as the analogous of a *critic*) with weights w . We will also assume that $\nu = \sum_{j=1}^M \delta_{y_j}$ is the distribution of all real points, and $\mu = \mathbb{P}_\theta$ is the distribution of $G_\theta(z)$, where G_θ is the *generator*, $z \sim p$, and p is the “noise” latent distribution. We independently pick a sequence of points x_i from \mathbb{P}_θ . We denote with $\mu_N = \sum_{i=1}^N \delta_{x_i}$ the **Nth-order empirical distribution** by summing the first N points. Finally for every generated point x , we define $y(x, w)$, as follows:

$$y(x, w) = \arg \inf_{y \in \text{supp}(\nu)} \{c(x, y) + \psi_w(y)\}. \quad (3.1)$$

For fixed (x, w) , $y(x, w)$ is the point that is assigned by the formula for the dual. As we will see in the appendix, this point is unique with probability one. If one point does not have a unique assignment then we arbitrary assign a point without loss of generality. By standard results in probability, we have that almost surely it holds $\mu_N \rightarrow \mu$, and therefore

$$\begin{aligned} & \mathbf{D}_w \left(\int \psi_w^{\text{supp}(\nu), c}(x) d\mu(x) - \int \psi_w(y) d\nu(y) \right)_{|w=w_0} \\ &= \int \mathbf{D}_w (\psi_w^{\text{supp}(\nu), c}(x))_{|w=w_0} d\mu(x) - \int \mathbf{D}_w (\psi_w(y))_{|w=w_0} d\nu(y) \\ &= \lim_{N \rightarrow \infty} \int \mathbf{D}_w (\psi_w^{\text{supp}(\nu), c}(x))_{|w=w_0} d\mu_N(x) - \int \mathbf{D}_w (\psi_w(y))_{|w=w_0} d\nu(y) \\ &= \lim_{N \rightarrow \infty} \mathbf{D}_w \left(\int (\psi_w(y(x, w)) + c(x, y(x, w))) d\mu_N(x) - \int \psi_w(y) d\nu(y) \right)_{|w=w_0} \\ &= \lim_{N \rightarrow \infty} \mathbf{D}_w \left(\frac{1}{N} \sum_{i=1}^N \psi_w(y(x_i, w)) - \frac{1}{M} \sum_{j=1}^M \psi_w(y_j) + \frac{1}{N} \sum_{i=1}^N c(x_i, y(x_i, w)) \right)_{|w=w_0}, \end{aligned} \quad (3.2)$$

where \mathbf{D}_w is the derivative with respect to w , in the first and third equality we applied Leibniz’s rule, and in the second equality we used the fact that $\mu_N \rightarrow \mu$. Since w_0 , is fixed, with probability one, we get that the last term in (3.2) is equal to

$$\begin{aligned}
 & \lim_{N \rightarrow \infty} \mathbf{D}_w \left(\frac{1}{N} \sum_{i=1}^N \psi_w(y(x_i, w_0)) - \frac{1}{M} \sum_{j=1}^M \psi_w(y_j) + \frac{1}{N} \sum_{i=1}^N c(x_i, y(x_i, w_0)) \right)_{|w=w_0} \\
 &= \lim_{N \rightarrow \infty} \mathbf{D}_w \left(\frac{1}{N} \sum_{i=1}^N \psi_w(y(x_i, w_0)) - \frac{1}{M} \sum_{j=1}^M \psi_w(y_j) \right)_{|w=w_0} \\
 &= \lim_{N \rightarrow \infty} \sum_{j=1}^M \left(\frac{\#\{x_i, 0 \leq i \leq N : y(x_i, w_0) = y_j\}}{N} - \frac{1}{M} \right) \mathbf{D}_w (\psi_w(y_j))_{|w=w_0},
 \end{aligned} \tag{3.3}$$

where in the (3.3) one can notice that y does not vary with w anymore, and that is why $\mathbf{D}_w \frac{1}{N} \sum_{i=1}^N c(x_i, y(x_i, w))$ vanishes. This happens because, for small changes in w , the assignments do not change with probability one. The proof of that claim can be found in the appendix.

This proves that the error functions

$$\int \psi_w^{supp(\nu), c}(x) d\mu(x) - \int \psi_w(y) d\nu(y) \tag{3.4}$$

and

$$\sum_{j=1}^M \left(\frac{\#\{x_i, 0 \leq i \leq N : y(x_i, w_0) = y_j\}}{N} - \frac{1}{M} \right) \psi_w(y_j), \tag{3.5}$$

where N is picked sufficient big, can be used interchangeably for the “critic”. We note that, by applying the theory of Large Deviations (see [7]), one can prove that the probability of the distance between the gradients of (3.4) and (3.5), being bigger than some ϵ , decays exponential with the number of N .

The cost appearing in (3.5), will be referred from now on as the Assignment cost, and it is the one that we used to train our Auxiliary network (“*assigner*”). In the next section we are going to further analyze the idea behind the Assignment cost and compare it with the *critic* cost in WGANs. We conclude with what we believe to be an interesting remark.

Remark 3.2 *By taking the derivative of (3.5) one gets*

$$\sum_{j=1}^M \left(\frac{\#\{x_i, 0 \leq i \leq N : y(x_i, w_0) = y_j\}}{N} - \frac{1}{M} \right) \mathbf{D}_w (\psi_w(y_j))_{|w=w_0}.$$

If all points x_i are assigned equally to every y , then the derivative is equal to zero and therefore the training halts. Although this would be sufficient for the generator to be trained, one can wonder if we end up with an optimal assignment between μ_N and ν . Trying to answer this question we came up with a theorem that confirms that.

More specifically we have

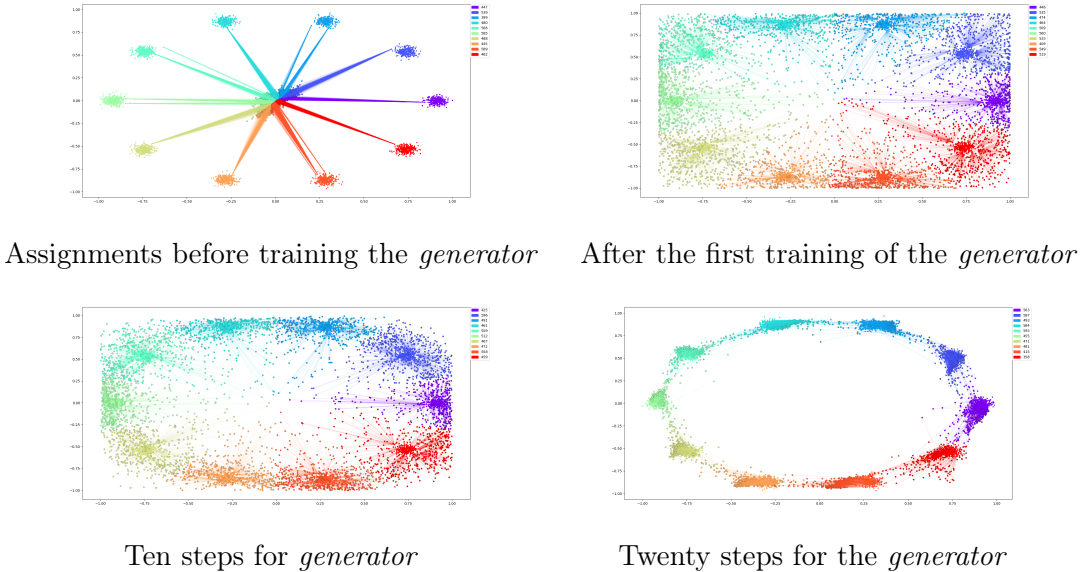


Figure 2: Visualization of the assignments of generated points, initially found in the middle, to a ring of gaussians.

Theorem 3.3 *Let $\mu, \nu \in \mathcal{P}(\mathcal{X})$, $\psi \in \mathcal{L}(\mu)$. We further assume that there exists a unique minimizer $\tilde{T}(x)$ of $\{c(x, y) + \psi(y)\}$, for μ almost every x . Then if $\tilde{T}_\# \mu = \nu$, we have that $(I \times \tilde{T})_\# \mu$ is an optimal plan.*

We note that, by Theorem 8.1, if μ is an absolutely continuous measure, ν is purely atomic, and c satisfies Assumption 3.1 then the map \tilde{T} is always defined. To reformulate, in order to know if ψ is a maximizer in the dual formulation for μ, ν , we only have to check that $\{c(x, y) + \psi(y)\}$, has a unique minimizer $\tilde{T}(x)$ for μ almost every x , and that minimizer satisfies $\tilde{T}_\# \mu = \nu$.

4 Analysis and comparison of the Assignment cost.

4.1 Assignment cost beyond its optimal transport origin

Even if one finds it hard to follow the derivation of (3.5) and its connection to optimal transport, the cost itself can be explained in a straight forward manner. We start by taking two sets of points $\mathcal{X}_1, \mathcal{X}_2$. For visualization purposes one can think \mathcal{X}_1 as the set of generated points and \mathcal{X}_2 as the set of real points. For each point x in \mathcal{X}_1 , we assign one point in set \mathcal{X}_2 , through the formula

$$y(x, w) = \arg \inf_{y \in \mathcal{X}_2} \{c(x, y) + \psi_w(y)\}. \quad (4.1)$$

Now, some real points in \mathcal{X}_2 have many generated points in \mathcal{X}_1 assigned to them, while at the same time, some others have no points assigned to them at all. For the real points that have many generated points assigned to them, we would like ψ_w to increase, and for

those who are under-assigned to decrease. The change to the values of ψ_w in a real point is weighted by the numbers of generated points assigned to it. Finally the $-1/M$ constant that appears in (3.5) can be understood as a normalization constant. The *assigner* ψ_w is trained to perfection, when all points are assigned equally.

When the *assigner* is trained to perfection, then one can use the assignments to send the generated points to the reals that are assigned. We would like to highlight that since the assignment is provided through the cost function, a perfectly trained *assigner* captures this information as well. This means that the image of the *generator* would be a manifold fitting the real data points but with a geometry that is inherited by the cost function.

4.2 Heuristic comparison between Assignment training and WGANs

Before we proceed with the comparison of the two methods, we would like to share a little bit from the history of our research for educational purposes. We believe that the following will help new researchers clarify some things about how WGANs work, and avoid our mistakes.

We start by, once more, reminding the reader about the dual formulation of the transport cost, i.e.

$$\mathcal{T}_c(\mu, \nu) = \sup_{\psi \in C_b(\mathcal{X})} \left\{ \int \psi^{supp(\nu), c} d\mu(x) - \int \psi d\nu(y) \middle| \psi^{supp(\nu), c}(x) = \inf_{y \in supp(\nu)} \{c(x, y) + \psi(y)\} \right\}. \quad (4.2)$$

Note that, in order to calculate the dual function of ψ , one has to go through **only** the points that are in the $supp(\nu)$ and not through the whole space \mathcal{X} . Our initial approach was to use small batches, in the same way that WGANs are traditionally trained, and with the hope that if the batches come closer then the full distributions of real and generated points will also come closer together. We note that in order to calculate the infimum in a differentiable way we applied a smooth maximum by using the LogSumExp function. Although this approach worked fine with low-dimension datasets having only a few nodes, it failed with datasets like MNIST. What we observed there was the production of blurred idealized versions of the digit.

Further experiments showed that an increase in the size of the batches for training both *generator* and *critic* positively increased the image quality. This lead us to believe that approximating the distance will only work when the number of samples is really high. When thinking of the problem as an optimal transport problem this becomes much clearer, as there is the possibility that samples from the closest manifold inside the data might not be in the batch we use for approximation. Furthermore if we think of each image from the MNIST dataset as a point in dimension $\mathbb{R}^{28 \times 28}$ of a probability distribution we would need significantly more samples to accurately capture a distribution or even find a sufficient approximation. As it was pointed out in [3, 4] this line of reasoning, i.e. if the batches come closer then the full distributions of real and generated points will also come closer together, for why WGANs *do* work, is not valid anyway. By applying a simple mass concentration argument, they show, that in order for this argument to be valid, one needs to increase the batch size exponentially with the number of dimensions. Something like that is of course impossible in practice.

In order to understand why the WGAN method works with small batches we came with the following visual explanation. When the *critic* is fed with some real points, its value there increases and when the *critic* is fed with some generated point the value there is decreases through the error function.

$$\sum_{x_i \sim \mathbb{P}_r} f(x_i) - \sum_{y_j \sim \mathbb{P}_\theta} f(y_j). \quad (4.3)$$

Then, roughly speaking, the trained *critic* is encoding a landscape where the generated points are valleys and the real ones are hills. The *generator* follows that landscape to "roll down" the generated points to the reals. The idea of the gradient penalty, apart from its mathematical justification, enforces this explanation scheme, because in practice, it smoothens the landscape along the lines between real and fakes. Therefore we hypothesized that it is not the fact that the batches really capture the two distributions, which makes WGANs work, but that:

- When the learning rate is small enough, then it makes no practical difference between applying 4.3 for many consecutive small batches or for a really big one. We believe that this is due to
 1. the linearity of the cost
 2. the fact that the *critic* network has enough degrees of freedom such that local changes do not significantly affect the rest of the network.
- The iteration between training the *critic* and the *generator*, is really necessary for the generated points to go closer to the real ones.

To test this perception, that it is not the *critic* cost (4.3) that in every step really captures the distance but the fact that when the learning rate is small enough, then it makes no practical difference between training the *critic* in many consecutive small batches or in a really big one, we trained WGANs with gradient penalty and with really small batches of 1 or 2 points. Given enough time, the result was almost as good as training with a batch of 64 or 128. At the same time, we also tried to train a perfect *critic* first and then train the *generator*, and this method failed even after thousand iterations of the *critic*.

Now if one wants to train with a general transportation cost using (4.2), this is not longer possible. In order for the dual of the *critic* to be defined properly then one has to go through a set of reals that capture well its distribution. If one tries to apply smaller batches the training fails.

For visual purposes, we would like to note that unlike in WGANs, in the Assignment method, the *assigner* never goes through the generated points. Furthermore, the *assigner* does not create a landscape where real points are high and generated points are low so the *generator* can use to train. In the assignment method, the *assigner* increases at real points which are assigned to too many generated points and decreases otherwise. When the *assigner* is trained to optimality then the training of the *generator* happens through the assignment and the cost that shapes the *assigner*.

5 Psudocode and comparison with WGANs

Algorithm 1 WGAN2. We use the parameters $\alpha = 0.00005$, $m = 10 * \text{len}(\mathcal{X})$, $n_{\text{critic}} = 5$.

Require: α is the learning rate. n_{critic} , the number of *assigner* iterations per *generator* iteration. m , the number of assignments per iteration of the *assigner*.

Require: w_0 , initial *assigner* parameters. θ_0 , initial *generator* parameters. \mathcal{X} , Matrix containing all of the real samples.

```

1: while  $\theta$  has not converged do
2:   for  $t = 0, \dots, n_{\text{critic}}$  do
3:     for  $i = 0, \dots, m$  do
4:       Sample latent space  $z \sim p(z)$ 
5:        $K^i \leftarrow (X[\text{argmin}(A_w(\mathcal{X}) + \text{cost}(\mathcal{X}, G_\theta(z))], G_\theta(z))$ 
6:        $L^i \leftarrow -A_w(K^i(0))$ 
7:     end for
8:      $w \leftarrow \text{RMSProp} \left( \mathbf{D}_w \left( \frac{1}{m} \sum_{i=1}^m L^i - \frac{1}{\text{len}(\mathcal{X})} \sum_{x \in \mathcal{X}} A_w(x) \right), w, \alpha \right)$ 
9:   end for
10:  for  $i = 0, \dots, m$  do
11:     $L^i \leftarrow \widetilde{\text{cost}}(K^i(0), K^i(1))$ 
12:  end for
13:   $\theta \leftarrow \text{RMSProp}(\mathbf{D}_\theta \frac{1}{h} \sum_{i=1}^h L^i, w, \alpha)$ 
14: end while

```

- Line 1: For all the tested cases, 100 iterations were enough for convergence. Furthermore, since the method allows to get an upper bound for the transportation cost distance, we can allow train until a specific error value is achieved.
- Line 3 and 10: These steps can be separated into multiple batches. For the first one, the best choice is to make it as big as the memory of the computer allows. For the second one, experiments show that optimal number is around 50.
- Line 4. Traditionally the latent distribution $p(z)$ is chosen to be a Gaussian. However we noticed that if we instead choose a collection of Gaussians with small variance the results are much better.
- Line 5 and 11: cost and $\widetilde{\text{cost}}$ need to coincide from the view of optimal transport. However, in practice, a computationally faster cost can be used for the *assigner*. It also appears that the *assigner* trains the fastest if we multiply the cost with a constant such that the diameter of the space is equal to one. This does not change the manifold of the resulting model (image of the *generator*).

5.1 Practical comparison between Assignment method and WGANs.

Advantages of Assignment method over WGANs.

1. It provides a quantitative way to bound from above the real distance between the distributions. As a byproduct, this allows to see how different parameters affect the training. For example, we noticed that with Fashion MNIST one gets the best approximation when latent dimension is around 250. Contrary, with the classical MNIST dataset, no significant difference appear if we increase the latent dimension further than 100.
2. We can approach the original distribution in any desirable degree.
3. The *assigner* can be trained to optimality by itself and without any iterations with the *generator*. This way we can calculate the transport distance between the two measures, and retrieve the optimal transport map.
4. It does not depend on the structure of the network. It can work well with the simple dense networks unlike the traditional WGANs.

Disadvantages of Assignment method over WGANs.

1. The training time is of order $O(N^2)$ where N is the number points in the original dataset.
2. It is relatively easy to overfit.

6 Experiments

In the following section, we describe the layout for the experiments that were conducted. We will start by introducing the datasets and giving an intuition why these datasets are useful to compare the performance of different approaches. Afterwards, we will define metrics that can evaluate the performance of the results.

6.1 Datasets

In this section, we will describe the datasets that were used for the experiment. We will state the preprocessing steps that were applied before using them as input and state the reasons why we choose them. We would like to note that we did not include the standard by now Cifar10 dataset, because we were not able to reproduce the claimed results of the other papers on this dataset at all. We believe that this was solely due to the architecture of the *generator*. We trained our model with a dense generator with a reasonably good outcome, but we decided not to include any images because of the lack of comparison. The interested reader, can use the code in the repository to check for themselves.

6.1.1 MNIST

The MNIST dataset is a collection of handwritten digits from 0 to 9 and labels indicating the number it should represent as an integer. The individual images consist of 28x28 greyscale values 70000 images are part of the dataset. For the experiments, we reduce the number of

images to 5000 examples upscale them to 32x32 and change the pixel values to be in the range of [-1,1].

The MNIST dataset is a typical dataset for comparing different GAN models because of their popularity in the machine learning community. Additionally, the numbers are easy to recognize and blurry images can be seen at a glance.

6.1.2 Fashion-MNIST

The fashion-MNIST dataset was created by Kashif Rasul and Han Xiao [15] as an alternative dataset to the MNIST. The fashion-MNIST is a collection of pictures of clothings. The number of classes is kept the same to MNIST that represent ten different clothing types. The individual images consist of 28x28 greyscale values and the number of examples in the dataset is 70000. For our experiments, we reduce the number of images to 5000 examples and upscale them to 32x32. We change the pixel values to be in range of [-1,1].

We chose this dataset for multiple reasons, first we can visually detect blur in the generated images by looking at the sharpness of transition between clothings and black background. Secondly we can see if details in the image get generated like prints on t-shirts, zippers and wrinkles. Third we think that its interesting to see difference between the results of MNIST compared to this dataset because their main dimensions and pixel ranges are the same.

6.2 Metrics

Evaluating the performance of generative models is a nontrivial task. In the case of images, we typically want visually appealing images that at the same time do not just reproduce the original dataset it was trained on. Theis et. al. [12] discussed the evaluation of generative image model and concluded that the no single evaluation metric is accurate but always depends on the application at hand. Similarly, Ali Borji [6] concluded, after reviewing 24 quantitative and 5 qualitative measures, that there is no universal measure between model performances. This leaves us with the task to choose appropriate metrics to compare our introduced approach to our reference Models. In the following, we are going to present the Wasserstein-1, the variance from optimal assignment.

6.2.1 Wasserstein-1 metric

The Wasserstein-1 distance will now be used as a metric for evaluating the generated samples after training. By calculating the distance for a large number of samples from the generator and the dataset we can approximate how close both distributions are to each other. For the experiments, we choose to sample ten times the amount of generated points compared to the size of the original dataset to get an accurate representation of the distance between our learned model and the dataset. To find the Wasserstein-1 metric we relied on the external library POT: Python Optimal Transport (see [8]) to solve the optimal transport problem that implements the algorithm proposed in "Displacement interpolation using Lagrangian mass transport" [5] by Bonneel et. al.

6.2.2 Assignment Variance

Apart from the Wasserstein-1 metric to determine how well the model has been trained we propose a metric that is depended on the cost function that the model uses. We evaluate with this metric how well a particular model achieves an equal spread of generated points around each of the real points in the dataset. To do this we take ten times the number of generated points compared to the amount of real points in the dataset. We then use the model specific cost function c and find the closest real point in the dataset. By counting how many generated points get assigned to a point in the real dataset we can determine if the model is spreading the points equally or if mode collapse is occurring in the model with respect to its cost c . Additionally this metric is independent of the dimension of a dataset points, allowing us to compare training results independently of the dataset.

To generate a single value we calculate the variance around the perfect result of ten assignments.

$$\frac{1}{\#reals} * \sum_{i=1}^{\#reals} \sqrt{(\#assignments_i - 10)^2} \quad (6.1)$$

6.3 Implementation and Hardware

As the main programming language Python3 was chosen for the project, the main reasons were that a lot of the major machine learning frameworks like Theano, Tensorflow and Pytorch are implemented in Python or have an easy to use API that can be used with python. Additionally, Python has multiple auxiliary libraries that help to implement machine learning libraries and evaluate results.

Tensorflow was chosen as the main framework. There was also the option to choose Theano and Pytorch as the framework, but a lot of the relevant gan approaches that are available in public git repositories. The main repositories we used as comparison that the implementations of GAN, WGAN and WGAN-GP were correct were.

- WGAN-GP : <https://github.com/ChengBinJin/WGAN-GP-tensorflow>
- GAN and WGAN : <https://github.com/wiseodd/generative-models>

All experiments were conducted on a Titan X Pascal GPU with 12 Gigabyte of GPU memory. Our repository for the experiment can be found in

- <https://github.com/artnoage/Optimal-Transport-GAN>.

7 Results and Discussion

7.0.1 MNIST

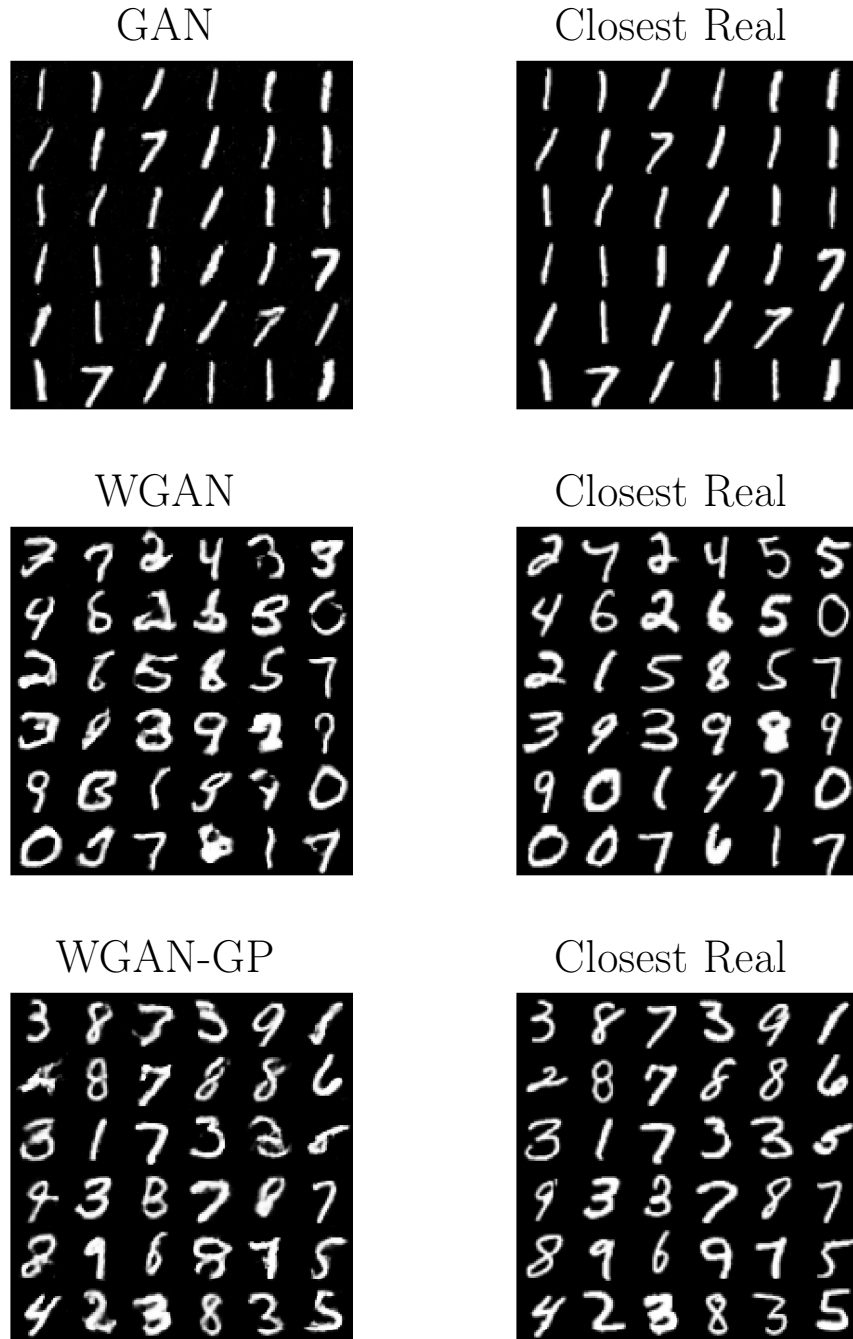


Figure 3: Generated samples for MNIST with GAN, WGAN and WGAN-GP. The closest real points were chosen by the cost function definition of the model. For vanilla GANs we used the Euclidean distance, since there is no cost function for this model.

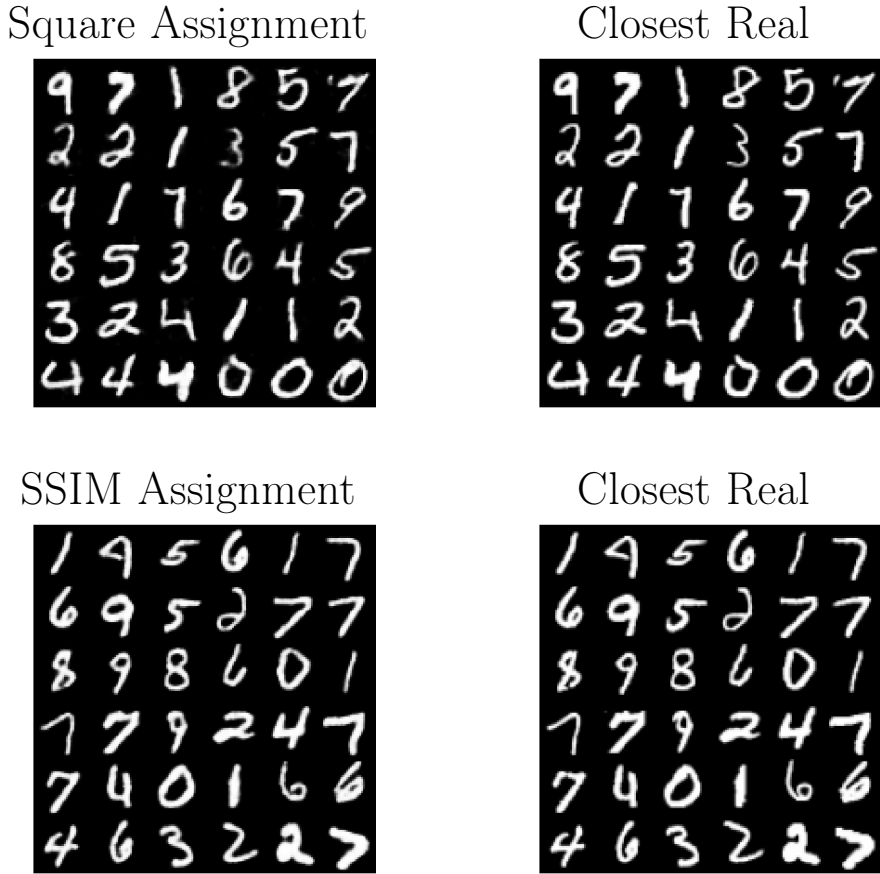


Figure 4: Generated samples for MNIST with the assignment approach. The closest real points were chosen with respect to the cost function defined by the model.

	GAN	WGAN	WGAN-GP	Square Assignment	SSIM Assignment
Wasserstein Metric	15.80	12.59	10.69	9.68	9.67
Assignment Variance		0.46	0.29	0.14	0.21

Table 1: Metrics applied on MNIST

We generated samples together with the closest real point based on the cost function of the method. Results from the models we use as comparison can be seen in figure 3 and our results can be seen in 4. The original GAN approach seems to only produce two rather similar looking numbers while the other approaches produce a larger variety of numbers. The quality of the images seems similar to us while a little bit sharper for our squared and SSIM Assignment. Additionally, we notice that WGAN, GAN-GP and the Square Assignment seem to produce numbers where pixels inside the lines of the numbers are missing or are not fully white while the SSIM Assignment generated images are fully connected. We think this behavior reflects the fact that SSIM optimizes for the structural integrity of the number as well as equal luminance and contrast. The Wasserstein metric in Table 1 reflects the perceived

image quality showing the best results for our method. Then looking at the numbers for the variance from optimal assignment we can see that our methods indeed managed to achieve their training objective the closest by having an equal spread around the dataset points. In conclusion one can say that the experiments for MNIST show what we expected, the square distance is able to move the model closer to the real distribution by having a smoother gradient when points get close while the SSIM Assignment manages to produce perceptual more appealing images.

7.0.2 Fashion MNIST

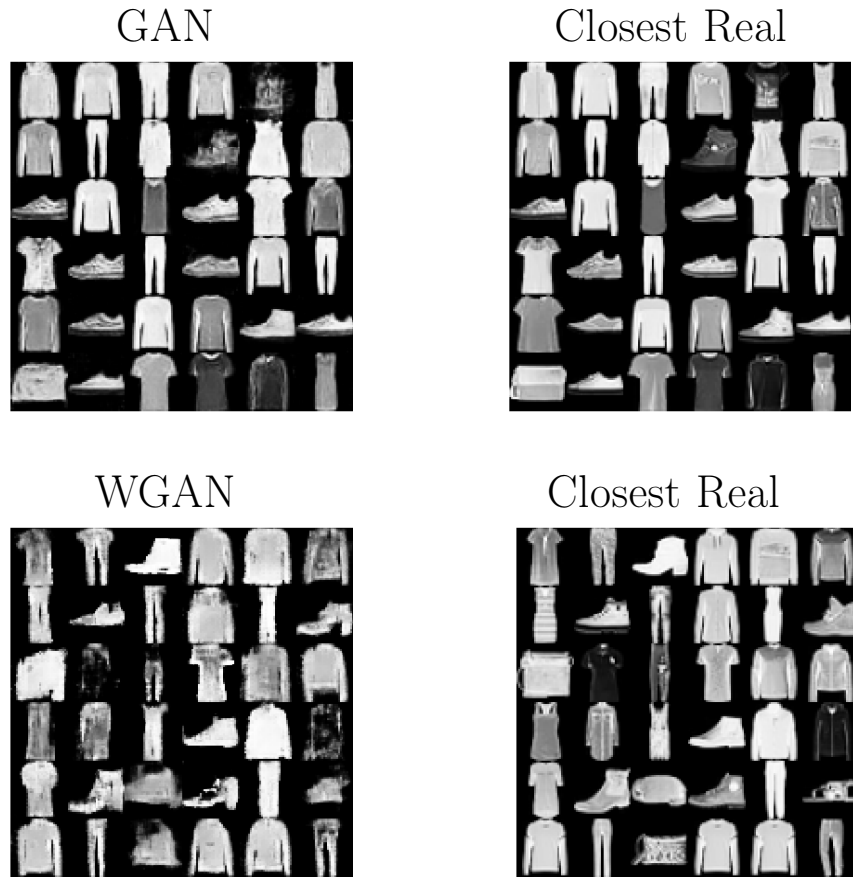


Figure 5: Generated samples for Fashion-MNIST with GAN, and WGAN. The real Closest Real points were chosen by the cost function definition of the model. For GANs we choose the Euclidean distance because there is no cost function for this model.

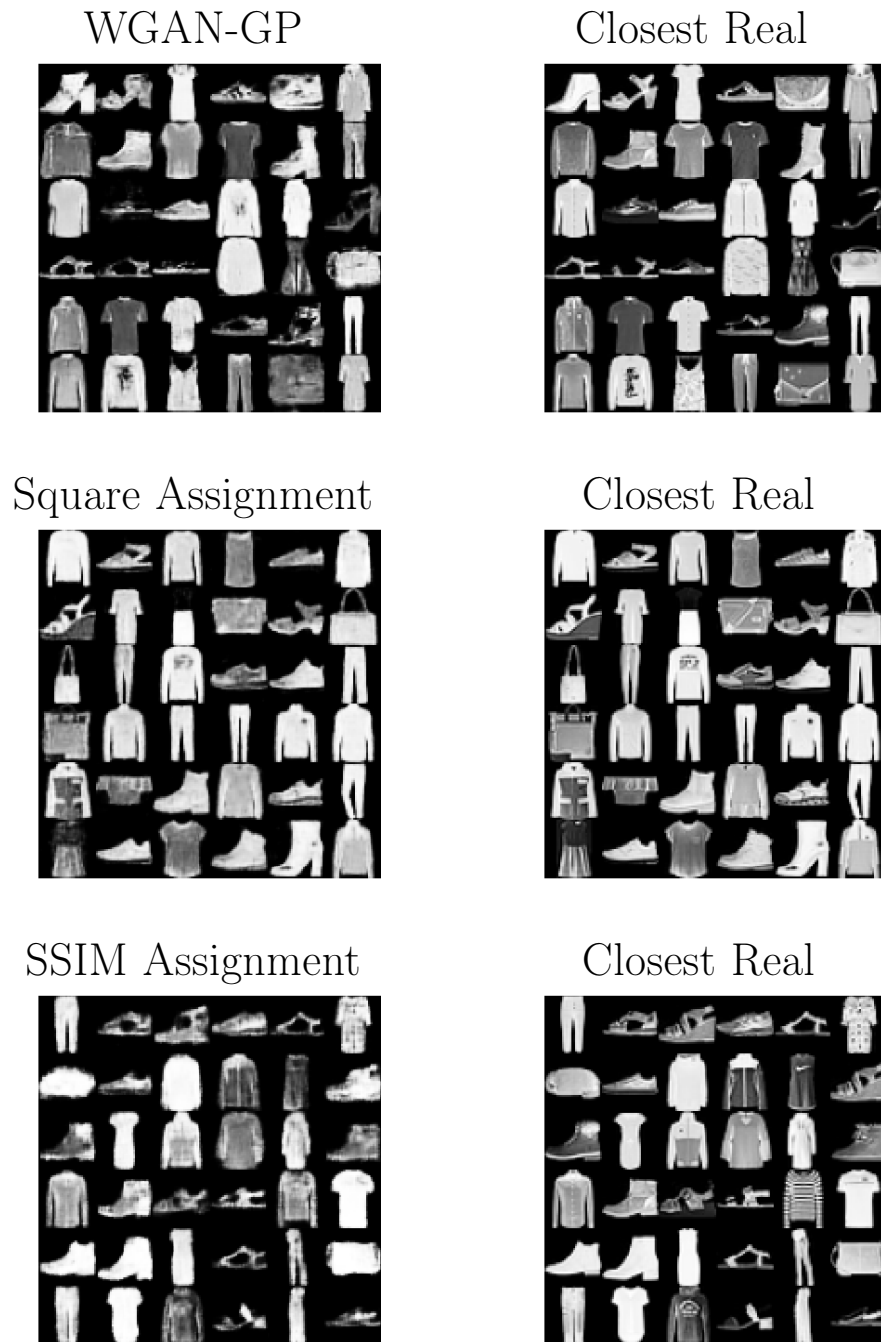


Figure 6: Generated samples for Fashion-MNIST for WGAN-GP, Square Assignment and SSIM assignment. The real Closest Real points were chosen by the cost function definition of the model.

To judge the visual quality, we can check the blurriness of the clothes at the edges of transition from the background and additionally can see if smaller details are present like prints on t-shirts, zippers and wrinkles. The results in figure 5 show the output of the models for comparison and 6 the results of our approaches. The overall visual quality of the images

	GAN	WGAN	WGAN-GP	Square Assignment	SSIM Assignment
Wasserstein Metric	11.03	11.19	9.15	3.40	7.17
Assignment Variance		1.99	0.82	0.01	0.05

Table 2: Metrics for the Fashion-MNIST

seems to be equal except for WGAN showing artifacts and general blurriness. This might show that clipping the weights of the network prevents it from learning the more complicated Fashion-MNIST distribution function. Additionally GAN seems to show no obvious mode collapse unlike with the classical MNIST. We interpret that discrepancy as an indicator that the original GAN is very sensitive to the choice of the hyperparameters, and we are in no way claiming that original GAN is not able to capture the MNIST dataset. Another observation is that all GANs and even WGAN-GP, are producing points that seem to be far different from the real dataset but at the same time look realistic suggesting that it learned a model that found some underlying representation of the dataset. When looking at the details inside the clothings one can see that WGAN-GP as well as our approach produces some but especially the Square Assignment is reproducing a lot of the details. When examining the metrics in Table 2 we can see that both of our approaches generate samples that are closer to the real distribution when calculating the Wasserstein-1 distance. When looking at the variance from optimal assignment one can see that how well the approach respectively achieves its objective is also reflected in the Wasserstein-1 distance. For the number of samples we drew the Square Assignment was able to perfectly place ten points close to each generated point.

7.1 Conclusion

We explored the idea of training GNs with various optimal transport costs. As the first cost we choose the squared Euclidean norm, that should have a smoother gradient for points that lie close to each other. The second cost was the structural similarity index proposed by [14] by Wang et. al. that tries to assess image quality by accounting for luminance, contrast and structure in the image that better reflect human perception of image quality. Choosing this cost allows us to train our generative model to train for generating images of high perceptual quality. To train generative models with these new costs a novel training procedure was introduced that allows us to use these costs but can be exchanged to train with any metric. The downside to this new way of training is that the computational effort for a training step increases with the number of points in the dataset one uses for training. Our experiments show that it is indeed possible to train a model with our proposed cost and decrease the distance between the generated points and the points in the dataset compared to approaches by other authors. Furthermore, the experiment results with the SSIM cost shows that the cost indeed influences the appearance of the generated images in some cases. The Wasserstein-1 metric applied on the results, further shows that we are able to better approximate the distribution of both MNIST as well Fashion-MNIST datasets when using the assigning approach.

Several possible research directions can build upon our work. There can be follow up work that tries to tackle the computational burden introduced by our approach. We think

that the largest improvement can be achieved by exploring more efficient ways to find the closest neighbours between the real and generated points that are necessary for our algorithm. Secondly one can try new costs that better reflect the training objective one tries to achieve. Especially with datasets where the Euclidean distance is a poor choice for assessing the similarity between data points. At last, one can look at the architecture choices made for the neural networks, the optimizers and the hyperparameters that might be more suitable for a given dataset and training objective.

8 Appendix

Theorem 8.1 *Let $\psi_w : \mathcal{X} \rightarrow \mathbb{R}$, a collection of functions parameterized by w . Let also assume that for every $y \in \mathcal{X}$, $\psi_w(y)$ is a continuous function with respect to w , and that c satisfies the Assumption 3.1. Finally, let \mathbb{P} be a distribution in \mathcal{X} , that is absolutely continuous with respect to the Lebesgue measure.*

For w_0 and a finite set Y , we have that for almost every $x \in \mathcal{X}$, the expression

$$\psi_{w_0}(y) + c(x, y)$$

has a unique minimizer in Y . Evermore with probability one, for every independent random sample, with respect to \mathbb{P} of points $\{x_1, \dots, x_n, \dots\}$ in X , we have that it exists $\delta(\{x_1, \dots, x_n\})$, such that

$$\arg \min_Y \{\psi_{w_0}(y) + c(x_i, y)\} = \arg \min_Y \{\psi_w(y) + c(x_i, y)\}, \quad \forall w \in B(w_0, \delta(\{x_1, \dots, x_n\})). \quad (8.1)$$

Proof. Let assume that the set $\tilde{\mathcal{X}}$, of all points that have multiple minimizers has positive Lebesgue measure. Then, since Y is finite, there exists at least one $y_0 \in Y$ such that $\tilde{\mathcal{X}}_{y_0}$ of the points that are minimizers for

$$\psi_{w_0}(y_0) + c(x, y_0)$$

has positive Lebesgue measure. From that, we can induce that the set

$$\{x \in \tilde{\mathcal{X}} : c(x, y_0) = \{\psi_{w_0}(y_0) + c(x_0, y_0)\} - \psi_{w_0}(y_0) = c(x_0, y_0)\},$$

where x_0 is an arbitrary but fixed point in $\tilde{\mathcal{X}}_{y_0}$, has positive measure. contradicts the assumption 3.1.

Now since the points x_1, \dots, x_n, \dots are sampled independently from \mathbb{P} , with probability one, the expression $\psi_{w_0}(y) + c(x_i, y)$, has unique minimizer $y(x_i)$, and further more it exists $\epsilon(x_i)$, such that

$$\psi_{w_0}(y) + c(x_i, y) > \psi_{w_0}(y(x_i)) + c(x_i, y(x_i)) + \epsilon(x_i), \quad \forall y \in Y \setminus \{y(x_i)\}. \quad (8.2)$$

Now if we pick $\delta(\{x_1, \dots, x_n\})$ such that

$$|f_w(y_i) - f_{w_0}(y_i)| < \min_{x_i} \epsilon(x_i),$$

we get the result. \blacksquare

We conclude with the proof of Theorem 3.3.

Proof of Theorem 3.3. Let Q be an optimal plan between μ and ν . By definition of \tilde{T} , we have

$$\psi(\tilde{T}(x)) + c(x, \tilde{T}(x)) = \psi^{\text{supp}(\nu), c}(x) = \inf_{y \in \text{supp}(\nu)} \{\psi(y) + c(x, y)\} \leq \psi(y) + c(x, y) \quad \forall y \in \text{supp}(\nu).$$

By integrating with respect to Q , we have

$$\int \psi(\tilde{T}(x)) + c(x, \tilde{T}(x)) dQ \leq \int (c(x, y) + \psi(y)) dQ,$$

which gives

$$\int \psi(\tilde{T}(x)) d\mu + \int c(x, \tilde{T}(x)) d\mu \leq \int \psi(y) d\nu + \int c(x, y) dQ.$$

Since $\tilde{T}_\sharp \mu = \nu$, the last inequality gives us

$$\int c(x, \tilde{T}(x)) d\mu \leq \int c(x, y) dQ,$$

which proves that \tilde{T} is an optimal map. \blacksquare

References

- [1] Martin Arjovsky, Soumith Chintala, and Léon Bottou. Wasserstein GAN. [arXiv preprint arXiv:1701.07875](https://arxiv.org/abs/1701.07875), 2017.
- [2] Martin Arjovsky, Soumith Chintala, and Léon Bottou. Wasserstein GAN. jan 2017.
- [3] S Arora, R Ge, Y Liang, T Ma, Y Zhang Proceedings of the 34th, and undefined 2017. Generalization and equilibrium in generative adversarial nets (gans). dl.acm.org.
- [4] Sanjeev Arora and Yi Zhang. Do GANs actually learn the distribution? An empirical study. jun 2017.
- [5] Nicolas Bonneel, Michiel van de Panne, Sylvain Paris, and Wolfgang Heidrich. Displacement interpolation using lagrangian mass transport. *ACM Trans. Graph.*, 30(6):158:1–158:12, December 2011.
- [6] Ali Borji. Pros and cons of gan evaluation measures. *Computer Vision and Image Understanding*, 179:41–65, Feb 2019.
- [7] A Dembo and O Zeitouni. *Large Deviations Techniques and Applications*, volume 38 of *Stochastic Modelling and Applied Probability*. Springer, New York, 2nd edition, 1987.

- [8] R'emi Flamary and Nicolas Courty. Pot python optimal transport library, 2017.
- [9] Ian Goodfellow, Jean Pouget-Abadie, Mehdi Mirza, Bing Xu, David Warde-Farley, Sherjil Ozair, Aaron Courville, and Yoshua Bengio. Generative adversarial nets. In Advances in neural information processing systems, pages 2672–2680, 2014.
- [10] Ishaan Gulrajani, Faruk Ahmed, Martin Arjovsky, Vincent Dumoulin, and Aaron C. Courville. Improved Training of Wasserstein GANs, 2017.
- [11] Huidong Liu, Xianfeng GU, and Dimitris Samaras. A Two-Step Computation of the Exact GAN Wasserstein Distance. ICML, pages 3165–3174, jul 2018.
- [12] Lucas Theis, Aäron van den Oord, and Matthias Bethge. A note on the evaluation of generative models. arXiv preprint arXiv:1511.01844, 2015.
- [13] Cédric Villani. Optimal transport: old and new. page 998, 2008.
- [14] Zhou Wang, A. C. Bovik, H. R. Sheikh, and E. P. Simoncelli. Image quality assessment: From error visibility to structural similarity. Trans. Img. Proc., 13(4):600–612, April 2004.
- [15] Han Xiao, Kashif Rasul, and Roland Vollgraf. Fashion-mnist: a novel image dataset for benchmarking machine learning algorithms. CoRR, abs/1708.07747, 2017.